

Synthesis, crystal structure, theoretical calculation and cytotoxic effect of new Pt(II), Pd(II) and Cu(II) complexes with pyridine-pyrazoles derivatives†

Elzbieta Budzisz,^{*a} Ingo-Peter Lorenz,^b Peter Mayer,^b Piotr Paneth,^c Lukasz Szatkowski,^c Urszula Krajewska,^d Marek Rozalski^d and Magdalena Miernicka^a

Received (in Montpellier, France) 16th May 2008, Accepted 1st July 2008

First published as an Advance Article on the web 10th September 2008

DOI: 10.1039/b808301k

The synthesis, structure and cytotoxic activity of Pt(II), Pd(II) and Cu(II) complexes of the general formula $MLCl_2$ ($M = Pt, Pd, Cu$) **2–4** and $(CuLCl_2)_2$ **5** where L is pyrazole-based chelate ligand 3-methyl-1-(2-pyridinyl)-1H-chromene[4,3-c]pyrazol-4-one **1** are described. The complexes were characterized by elemental analysis, infrared and 1H NMR spectroscopy, as well as electrospray mass spectrometry. Compounds **3** and **5** were also studied using X-ray diffraction. In addition, geometries, partial atomic charges, and lipophilicity, which determines their ability to penetrate through cells membranes, were obtained computationally. Complexes **2–4** exhibit square-planar geometries around the metal(II) centers and adopt *cis* configuration. Complex **5** is a dimer with distorted tetragonal pyramidal configuration at both Cu(II) centers, which are connected by two μ_2 -chloro bridges in axial positions. The cytotoxic effect of these complexes was examined on HL-60 and NALM-6 human leukemia cells and melanoma WM-115 cells. The Pt-complex *cis-2* exhibited moderate cytotoxic activity against leukemic cells, but relatively high activity toward melanoma cells with cytotoxicity of $IC_{50} = 16.6 \mu M$ at a level comparable to that of cisplatin ($18.2 \mu M$).

Introduction

Malignant melanoma (*melanoma malignum*) is known to be one of the most aggressive types of tumor, which is often difficult to treat. It stands for 1.5–2% of all diagnosed cases of cancer.¹ The standard methods of treatment of malignant melanoma are surgical oncology, radiotherapy (RTH), cryotherapy, photodynamic therapy (PTD),² and chemotherapy. Chemotherapy is the less often used kind of treatment, but it seems to be necessary in case of metastasis or after surgery to prevent micrometastasis.³ The most active cytostatic agent against melanoma is dacarbazine.⁴ Other partly active drugs against malignant melanoma are temozolomide, cisplatin, carboplatin, vinblastine, vincristine, paclitaxel and docetaxel.⁵ Cisplatin is often used in multidrug therapy, for example in CVD scheme (cisplatin, vinblastine

and dacarbazine) or PCV scheme (procarbazine, cisplatin, vincristine).⁶

In recent years, considerable attention has been paid to pyrazoles, pyrimidines and related *N*-containing heterocyclic derivatives.⁷ Systems of this kind play a significant role in many biological processes, due to their coordination ability for trace metal ions.⁸ Platinum–pyrimidine/pyrazole complexes which have demonstrated antitumor activity are an interesting class isolated from the reaction of cisplatin with pyrimidines and pyrazoles.⁹

Most ligands are based on nitrogen-containing heterocyclic compounds with exception of a few having sulfur and oxygen moieties. The key feature of these heterocycles is their π -electron deficiency. This is a common feature with bi- and tridentate nitrogen-based heterocyclic compounds such as 1,10-phenanthroline and 2,2'-bipyridine. Pyrazoles are widely studied five-membered heterocyclic compounds. Pyrazole derivatives exhibit antitumor, antiinflammatory, analgesic, antipyretic,¹ antimicrobial,¹⁰ anticoagulant,¹¹ and agrochemical¹² activity. Pyrazoloquinoline derivatives, which interact with the central benzodiazepine receptors are important tools for finding out the physiological properties and the structural requirements of the recognition site of the receptor itself.¹³

Second-generation platinum complexes possess “non-leaving ligands”, other than ammonia, and these are of interest for their ability to modulate drug metabolism and target binding through steric and electronic effects on the substitution mechanism.¹⁴ Several platinum complexes with *N*-heterocyclic ligands

^a Department of Cosmetic Raw Materials Chemistry, Faculty of Pharmacy, Medical University of Lodz, Muszynskiego 1, 90-151 Lodz, Poland. E-mail: elora@ich.pharm.am.lodz.pl; Fax: +48 42 678 83 98; Tel: +48 42 677 91 25

^b Department of Chemistry and Biochemistry, Ludwig Maximilian University, Butenandstr. 5-12 (D), D-81377 Munich, Germany

^c Institute of Applied Radiation Chemistry, Department of Chemistry, Technical University of Lodz, Zeromskiego 16, 90-924 Lodz, Poland

^d Department of Pharmaceutical Biochemistry, Faculty of Pharmacy, Medical University of Lodz, Muszynskiego 1, 90-151 Lodz, Poland

† Electronic supplementary information (ESI) available: Table 1S: Bond distances (Å) and angles (°) of complexes **3** and **5**. CCDC reference numbers 664742 (**3**) and 664743 (**5**). For ESI and crystallographic data in CIF or other electronic format see DOI: 10.1039/b808301k

such as benzimidazole, benzoxazole, imidazole, thiazole or benzoxazole have been reported. Some of them have shown significant cytotoxicity.¹⁵

Bidentate ligands used instead of ammonia could lead to prevention of translabilization and undesired displacement of the non-leaving ligand by sulfur and nitrogen donors that are present in the cell.

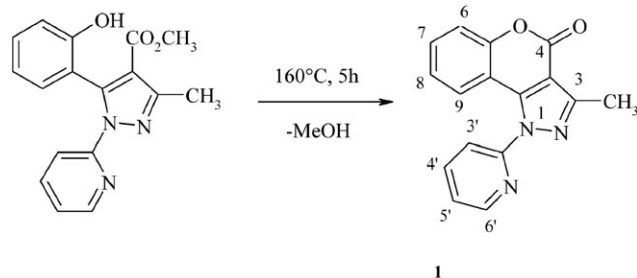
In our recent paper we have reported the synthesis and biological activity of the complex of 3-(1-aminoethyl)-4-hydroxychromen-2-one with palladium(II) where the environment of the Pd atom is similar to that in carboplatin.¹⁶ This complex has a 7800-times higher cytotoxicity than carboplatin. The present contribution reports three newly prepared platinum(II), palladium(II) and copper(II) complexes of the general formula $MLCl_2$ where L are pyrazolocoumarin ligands. Synthetic, structural and preliminary biological studies have been carried out. We also used quantum chemical calculations to evaluate stabilities of the obtained complexes, as well as their lipophilicity and electronic density distribution on atoms that participate in coordination. The lipophilicity is one of the most important factors for design of new drugs.¹⁷ Structure–cytotoxicity relationship studies revealed that for many compounds increased lipophilicity is often accompanied by increased cytotoxicity.¹⁸

Results and discussion

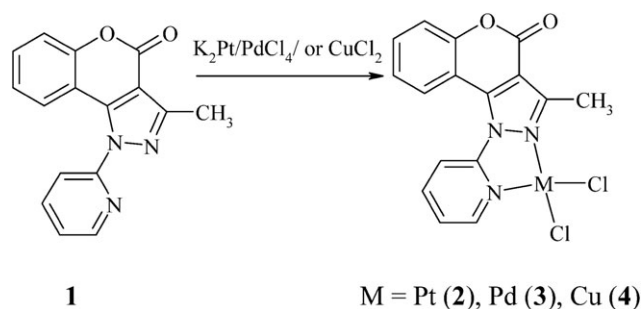
Chemistry

Preparation of the ligand. The target ligand **1** was synthesized according to the procedure described in our recent paper.¹⁹ 5-(2-Hydroxybenzoyl)-3-methyl-1-(2-pyridinyl)pyrazol-4-carboxylic acid methyl ester easily cyclizes under basic conditions in the reaction with nitrogen nucleophiles such as *N*-methylhydrazine to form 3-methyl-1-(2-pyridinyl)-1*H*-chromene[4,3-*c*]pyrazol-4-one (**1**). Thermogravimetric analysis of the copper complex described in our recent paper²⁰ confirmed detachment of methanol molecule and DMF. Detachment of methanol molecule could suggest the cyclization of pyrazole ligand to the coumarin derivative. According to these data we successfully performed the thermal cyclization of pyrazole ligand to its coumarin derivative **1** (see Scheme 1).

Synthesis of complexes. The complexes **2** and **3** of formula $MLCl_2$ were obtained by treatment of the ligand **1** with the salts K_2PtCl_4 or K_2PdCl_4 in a 1 : 1 ratio in water and methanol. Complex **4** was synthesized from $CuCl_2 \cdot 2H_2O$ in ethyl acetate (see Scheme 2).



Scheme 1 Synthesis of ligand **1** by cyclization.



Scheme 2 Synthesis of complexes **2–4**.

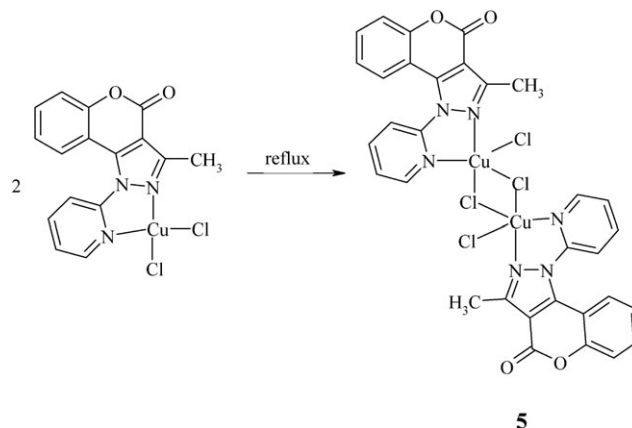
We have described two different methods for synthesizing the copper(II) complexes. The complex **4** was not formed in the methanolic solution, most likely due to methanolysis as we instead isolated the free ligand **1**. We instead obtained the complex **4** in the reaction of **1** with $CuCl_2 \cdot 2H_2O$ in ethyl acetate at room temperature. Under these conditions the methanolysis or hydrolysis is not possible and the complex was formed. Upon using higher temperature dimer **5** was formed (Scheme 3).

The IR spectra of the complexes are similar to those of the free ligand. The most characteristic bands are those at 1615 cm^{-1} attributed to $\nu(C=N)$ of the pyrazolyl group. The IR spectra of the complexes in the region $500\text{--}300\text{ cm}^{-1}$ were also recorded and show a well-defined band corresponding to $\nu(M-Cl)$ at $300\text{--}350\text{ cm}^{-1}$. Bands attributable to $\nu(M-N)$ at $450\text{--}490\text{ cm}^{-1}$ are also present.

Fig. 1 shows the 1H NMR spectra of aromatic regions of ligand **1** and complexes **2** and **3**. Signals for aromatic protons are at δ 7.20–8.80 ppm. The spectra are similar and we do not see the influence of coordination on shifts of the signals. The aromatic regions are detailed in the Experimental section and the atom numbering is shown in the Scheme 1. Signals for methyl protons of the ligand are at δ 2.575 and for complexes **2** and **3** are at δ 2.573 and 2.572, respectively (not shown).

X-Ray crystal structure analyses

X-Ray diffraction quality single crystals of **3** and **5** were obtained by vapor diffusion of ethyl acetate into DMF solutions of the complexes. The molecular structures of complexes **3** and **5** with the atomic numbering scheme are shown in Fig. 2



Scheme 3 Synthesis of complex **5**.

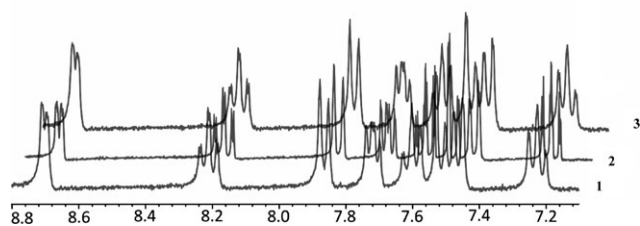


Fig. 1 ^1H NMR spectra of the ligand **1** and of complexes PtLCl_2 (**2**) and PdLCl_2 (**3**).

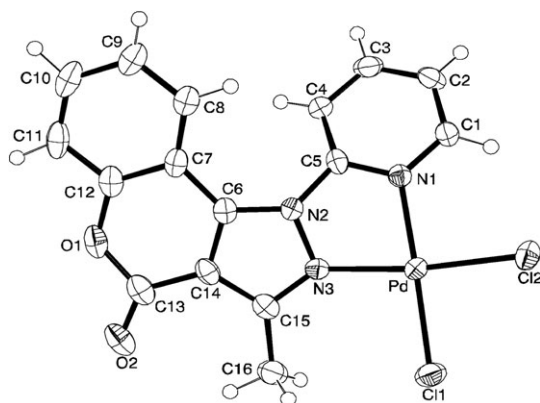


Fig. 2 Molecular structure of the palladium(II) complex **3**. Thermal ellipsoids of 30% are shown.

and **3**, respectively, and selected bond lengths and angles are given in Table 1S (ESI †). The configuration of Pd(II) in **3** is square-planar, formed by the two nitrogen atoms, N1 and N3, and two chloro ligands in *cis*-positions. The corresponding Pd–N and Pd–Cl bonds are almost equal, whereby both Pd–N distances (*ca.* 204 pm) are longer than those previously found by us in a similar complex (196 pm).²¹ The chelating angle N1–Pd–N3 ($79.95(8)^\circ$) is about 10° smaller than that of Cl1–Pd–Cl2 ($88.96(3)^\circ$). Because of the methyl group in the α -position to N3 the angle Cl1–Pd–N3 ($97.80(6)^\circ$) is larger than Cl2–Pd–N1 ($93.39(6)^\circ$). All atoms of **3** (Pd, Cl, C, N and O) are co-planar.

The dimeric Cu(II) complex **5** exhibits a distorted tetragonal pyramidal configuration at each Cu(II) center, where the two nitrogen atoms, N2 and N3, of the chelate system, and the

chlorido ligands, Cl1 and Cl2, form the plane and Cl2ⁱ lies in the axial position. Both $\mu\text{-Cl}$ bridges are unsymmetrical with two different Cu–Cl distances (Cu–Cl2 223.08(9) and Cu–Cl2ⁱ 267.27(10) pm). The Cu–N bonds are also quite different (Cu–N2 199.5(3) and Cu–N3 208.8(3) pm). The distortion is caused by the two N–Cu–Cl angles in *trans*-position (N2–Cu–Cl1 $150.21(8)^\circ$ and N3–Cu–Cl2 $172.31(8)^\circ$) as well as by all *cis*-angles (N2–Cu–N3 $78.51(10)^\circ$, Cl1–Cu–Cl2 $94.48(4)^\circ$ within the plane and Cl1–Cu–Cl2ⁱ $101.14(3)^\circ$, N2–Cu–Cl2ⁱ $106.94(8)^\circ$, N3–Cu–Cl2ⁱ $87.43(8)^\circ$ from the plane to the axial Cl2ⁱ-position).

Computational analysis. Superior performance of the mPW1PW91/LanL2DZ theory level in comparison with other DFT functionals for the calculation of geometries and vibrations for cisplatin and carboplatin has been well documented in the literature.²² This level was, therefore, used for the optimization of geometries in the gas phase. Results of these calculations are collected in Table 1 and compared with the crystallographic data available for Cu(II) and Pd(II) complexes. Atom numbering is presented in Fig. 2 on the example of the palladium complex. It is worth noting that the conformation of the free ligand is somewhat different than when ligated with the metal. The main geometrical parameter indicating this difference is the N1–C5–N2–N3 dihedral angle. It is close to *cis* conformation in the complexes, somewhat distorted by the nonplanarity resulting from the steric crowdedness, while it is much closer to the *trans* conformation in the free ligand.

Comparison of the calculated geometry of the palladium complex with the structure obtained from the X-ray diffraction (see Fig. 4) indicates excellent agreement between the experimental data and the computational result. In the case of the copper complex the agreement is less favorable, especially in the vicinity of the metal atom, although it is still very good as can be seen from data collected in Table 1.

In calculations incorporating solvents, we have used B3LYP/LACVP** theory level together with the PB solvent model with parameters for water and for 1-octanol. Values of $\log P$ values were then calculated from the free Gibbs energies. These energies are very sensitive to a single parameter for solvent, namely solvent radius (R_{solv}). Therefore, we have calibrated calculations of $\log P$ using cisplatin ($\log P = -2.27$) and *cis*-dichlorodicyclopentylamineplatinum(II) ($\log P = 1.06$) as standards.²³ As a result, for further calculations

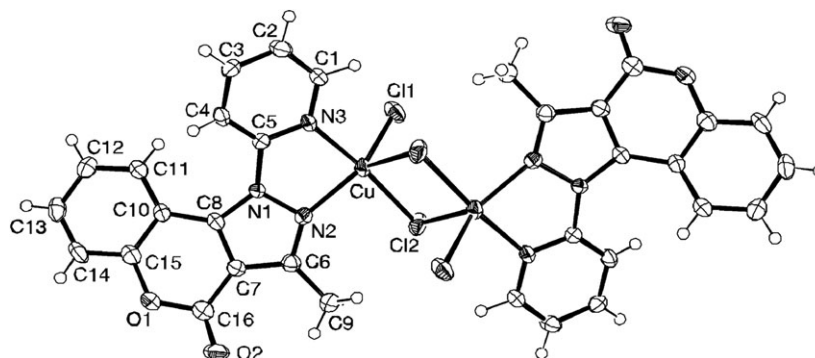
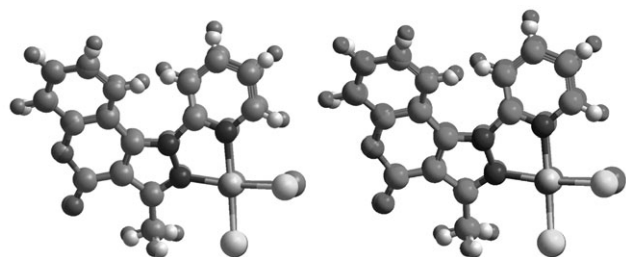


Fig. 3 Molecular structure of the dimeric copper(II) complex **5**. Thermal ellipsoids of 30% are shown.

Table 1 Selected geometrical parameters ($^{\circ}$ and \AA) obtained from DFT calculations at the mPW1PW91/LanL2DZ theory level

Compound	N1–M	N3–M	N1–M–N3	M–Cl2	M–Cl1	Cl1–M–Cl2	N1–C5–N2–N3	C7–C6–N2–C5
L (1)	—	—	—	—	—	—	–141.2	–10.6
LCuCl ₂ (4)	2.103	2.092	77.6	2.276	2.272	101.1	–26.1	–20.8
(LCuCl ₂) ₂ (5) (X-ray)	2.089	1.995	78.5	2.251	2.231	94.5	–25.8	–32.3
LPdCl ₂ (3)	2.081	2.087	78.9	2.367	2.359	90.4	–24.0	–24.4
LPdCl ₂ (3) (X-ray)	2.036	2.044	79.9	2.278	2.276	89.0	–27.9	–19.4
LPtCl ₂ (2)	2.046	2.039	79.5	2.396	2.390	89.0	–20.4	–26.0

**Fig. 4** Superposition of the structures of complex **3** obtained from DFT calculations and X-ray diffraction.

we have selected the value of R_{solv} equal to 0.2 because it yielded values of $\log P$ for these two compounds closest to the experimental data; –1.89 and 1.25, respectively. We were unable to optimize copper complexes in the 1-octanol model and in case of the dimer also using the model of aqueous solution. However, the energy differences resulting from the differences in geometries upon reoptimization in the condensed phase are very small; 0.04 and 0.20 for palladium and platinum, respectively. This confirms our previous conclusion that reoptimization using the solvent model is not necessary. In Table 2 main solvation energies and the resulting $\log P$ values are collected. The differences in solvation energies are up to 10 kcal mol^{–1} for all three metals.

Three different schemes of obtaining partial atomic charges were compared. Table 3 summarizes the partial atomic charges on the nitrogen, oxygen and hydrogen atoms obtained from Mulliken,²⁴ NPA,²⁵ and electrostatic fitting (ESP) analysis using the Merz–Kollman scheme.²⁶ As can be seen, partial atomic charges depend significantly on the population analysis scheme. Charges obtained from the electrostatic potential fitting seem to be best balanced. Furthermore, they were found to be closest to experimental results of charge transfer complexes.²⁷ We have, therefore, used them in the analysis of charges on the metal atoms in the studied complexes. The partial atomic charge on chlorine atoms diminishes from Cu to

Table 3 Partial atomic charges (δ) calculated at the BP/B3LYP/LACVP** level of theory

Compound	$\delta(\text{N1})$	$\delta(\text{N3})$	$\delta(\text{M})$	$\delta(\text{Cl})^a$
L (1)	–0.09	–0.13	—	—
LPtCl ₂ (2)	–0.41	–0.36	0.31	–0.34
LPdCl ₂ (3)	–0.30	–0.24	0.23	–0.40
LCuCl ₂ (4)	–0.39	–0.27	0.40	–0.45

^a Values averaged for two chlorine atoms.

Pd to Pt. Changes on nitrogen atoms as well as between aqueous and 1-octanol solutions are very minor. No systematic changes on the partial atomic charges on the metal atoms were observed.

Geometric features of all three complexes are quite similar (see Table 4). The N···M bond lengths are slightly longer in the nonpolar solvent while the opposite is true for the M···Cl bonds.

Cytotoxicity studies

The cytotoxicity of the complexes **2–5** and the ligand **1** was assayed against human HL-60 and NALM-6 leukemia cells and melanoma WM-115 cells. Cisplatin and carboplatin were used as reference compounds. Cells were exposed to a broad range of drug concentrations (10^{-7} – 10^{-3} M) for 48 h and cell viability was analyzed by MTT assay. IC₅₀ values are presented in Table 5. The Pt-complex **2** exhibited the highest cytotoxic activity with IC₅₀ values in the range of 16–34 μM for three cell lines. Interestingly, compound **2** was at least as effective against human skin melanoma WM-115 cells as the reference drug cisplatin. Because compound **2** seemed to be promising as an anticancer agent, its cytotoxicity was also assayed against normal HUVEC cells and unfortunately this was also high with IC₅₀ = 7.3 ± 0.6 μM . Cytotoxicity results strongly support the view that the observed cytotoxicity can be confidently attributed to the presence of the metal centers.

Table 2 Values of $\log P$ calculated from solvation free energies obtained at the B3LYP/LACVP** theory level using CPCM continuum solvent model

Compound	Gas-phase Gibbs free energy ^a /a.u.	Solvation free energy/kcal mol ^{–1}		
		1-Octanol	Water	$\log P$
L (1)	–930.876537	–12.55	–15.06	–1.82
LPtCl ₂ (2)	–1080.046337	–34.51	–37.02	–1.82
LPdCl ₂ (3)	–1087.623327	–33.88	–37.65	–2.73
LCuCl ₂ (4)	–1157.036660	–41.16	–46.62	–3.95
(LCuCl ₂) ₂ (5)	–2314.052101	–57.35	–67.48	–7.33

^a Obtained at the mPW1PW91/LanL2DZ level.

Table 4 Basic geometric features (Å, °) calculated at the BP/B3LYP/LACVP** level of theory

Compound	N1–M	N3–M	N1–M–N3	M–Cl2	M–Cl1	Cl1–M–Cl2	N1–C5–N2–N3	C7–C6–N2–C5
L (1)	—	—	—	—	—	—	–128.5	8.6
LCuCl ₂ (4)	2.050	2.045	79.9	2.322	2.322	95.8	–25.2	–22.3
LPdCl ₂ (3)	2.063	2.071	79.3	2.411	2.411	88.8	–25.2	–25.3
LPtCl ₂ (2)	2.040	2.031	79.6	2.440	2.440	87.5	–21.7	–26.9

Table 5 Cytotoxic activity of ligand 1 and its Pt, Pd and Cu complexes 2–5 (IC₅₀ in μM)

Compound	HL-60	NALM-6 IC ₅₀ ^a	WM-115
1	>1000	>1000	—
2	28.9 ± 9.3	34.0 ± 7.3	16.6 ± 3.9
3	543.5 ± 61.3	410.3 ± 52.1	135.6 ± 27.5
4	387.1 ± 31.7	545.4 ± 38.6	66.3 ± 2.3
5	178.2 ± 42.9	352.9 ± 42.7	—
Cisplatin	0.8 ± 0.1	0.7 ± 0.3	18.2 ± 4.3
Carboplatin	4.3 ± 1.3	0.7 ± 0.2	422.2 ± 50.2

^a These data are expressed as the means ± SD (*n* = 12). IC₅₀ = concentration of a tested compound required to reduce the fraction of surviving cells to 50% of that observed in the control, non-treated cell.

Lipophilicity is one the most important factors that has influence on a drugs' biological activity.²⁸ The complex 2 has the highest log *P* value (–1.82) and exhibits the highest cytotoxicity among the investigated complexes. However, the another important factor is the stability of compound. As we know, Pd(II) complexes present high lability and fast hydrolysis (10⁵–10⁷ faster in comparison to Pt(II) complexes).²⁹ Therefore, the higher cytotoxicity of complex 2 could be also connected with slower hydrolysis of Pt–Cl bond and the stability of this compound.

Conclusions

In this paper we have shown a simple and convenient route for synthesis of neutral *cis*-oriented Pt, Pd and Cu-complexes of general MCl₂ type. The structures of complexes 3 and 5 have been confirmed using X-ray diffraction. The complexes exhibit square-planar (3) or square-pyramidal (5) geometries around the Pd(II) or Cu(II) centers, respectively. 5 exists as a dimer. The results clearly indicate coordination *via* *N*-pyrazolic and *N*-pyridinic heteroatom.

The present study demonstrates that the Pt(II) complex 2 with the pyridine-pyrazole ligand 1 exhibits relatively high cytotoxic activity towards HL-60 and NALM-6 leukemia cells. Especially interesting is its activity against the WM-115 melanoma cell line, which is comparable with the activity of cisplatin and much higher than the activity of carboplatin. Unfortunately, the cytotoxicity of the complex 2 was also high against normal HUVEC cells. Pd(II) and Cu(II) complexes 3, 4 and 5 exerted rather low cytotoxicity against leukemia and melanoma cell lines. Ligand 1 was practically inactive. The computational analysis, carried out at the BP/B3LYP/LACVP**//mPW1PW91/LanL2DZ theory level, indicates that log *P* seems to correlate with the biological activity only for metal complexes, but not for the ligand. The highest cytotoxicity of compound 2 could be connected with the best

log *P* value, but also with slower hydrolysis of Pt–Cl bonds in comparison to Pd–Cl and Cu–Cl ones.

Experimental

Materials and methods

Potassium tetrachloroplatinate(II) and potassium tetrachloropalladate(II) were purchased from Aldrich and were used without further purification. Chloroform-*D* solvent for NMR spectroscopy was obtained from Dr Glaser AG Basel. Solvents for synthesis (toluene, methanol, dimethylformamide, acetone) were reagent grade or better and were dried according to standard methods. The melting points were determined using an Electrothermal 1A9100 apparatus and they are reported as uncorrected values. The IR spectra were recorded on a Pey-Unicam 200G Spectrophotometer in KBr or CsI. The ¹H NMR spectra were recorded using a 300 MHz Varian Mercury spectrometer. The MS data were obtained on a LKB 2091 mass spectrometer (70 eV ionisation energy) and the ESMS were recorded on a 5989A mass spectrometer with 59980B particle beam LC/MS interface (Hewlett-Packard). For new compounds satisfactory elemental analyses (±0.4% of the calculated values) were obtained in the Microanalytical Laboratory of the Department of Bioorganic Chemistry (Medical University, Lodz) using a Perkin–Elmer PE 2400 CHNS analyser. The ligand: 3-methyl-1-(2-pyridinyl)-1*H*-chromene[4,3-*c*]pyrazol-4-one (1) and Cu-complex (4) were prepared according to published methods¹⁹ or by thermal cyclization, in which 5-(2-hydroxybenzoyl)-3-methyl-1-(2-pyridinyl)-pyrazol-4-carboxylic acid methyl ester was heated for 5 h at 160 °C.

Syntheses of the complexes

Platinum(II) complex (2). An aqueous solution (5 mL) of K₂[PtCl₄] (41.5 mg, 0.10 mmol) was added dropwise to a stirred methanol solution (10 mL) of ligand 1 (28 mg, 0.10 mmol). The reaction mixture was stirred for 48 h at room temperature, and then half of the volume of the solvent was removed under reduced pressure at room temperature. A yellow precipitate of the product was obtained after 3 h. The crude solid was filtered off and dried under reduced pressure over CaCl₂; 22 mg (40% yield), mp 391.3–393.7 °C, IR spectrum in CsI, selected bands, cm^{–1}: 1744 (C=O), 1617 (C=N), 487 (Pt–N), 329 (Pt–Cl). ¹H NMR (DMSO-*d*₆) δ (ppm): 2.573 (s, 3H, CH₃), 7.201 (s, 1H, C(6)H), 7.442 (d, 1H, C(7)H), 7.469 (d, 1H, C(8)H), 7.600 (t, 1H, C(9)H), 7.634 (t, 1H, C(3')H), 7.851 (d, 1H, C(4')H), 8.204 (t, 1H, C(5')H), 8.708 (d, 1H, C(6')H). MS-FAB (*m/z*): 543 (100%), [Pt(L)Cl₂]; 373 (20%), [Pt(L)]²⁺. Anal. Calc. for C₁₆H₁₁N₃O₂PtCl₂ (543.2 g mol^{–1}): C 35.37, H 2.04, N 7.74. Found: C 35.14, H 2.23, N 7.51.

Palladium(II) complex (3). An aqueous solution (2 mL) of $K_2[PdCl_4]$ (0.1 mmol, 33 mg) was added dropwise to a stirred methanol solution (10 mL) of ligand **1** (0.1 mmol, 28 mg) at room temperature. During the addition the solid product was precipitated immediately from the reaction mixture. Stirring was continued for 30 min. The stable yellow complex was filtered off, washed with cold water, diethyl ether, and dried; 41 mg yield (90%), mp 369.7–371.3 °C, IR spectrum in CsI, selected bands, cm^{-1} : 1744 (C=O), 1615 (C=N), 458 (Pd–N), 347 (Pd–Cl). 1H NMR (DMSO- d_6) δ (ppm): 2.572 (s, 3H, CH_3), 7.200 (s, 1H, C(6)H), 7.446 (d, 1H, C(7)H), 7.468 (d, 1H, C(8)H), 7.604 (t, 1H, C(9)H), 7.709 (t, 1H, C(3')H), 7.877 (d, 1H, C(4')H), 8.203 (t, 1H, C(5')H), 8.708 (d, 1H, C(6')H). MS-FAB (m/z): 419 (80%), $[Pd(L)Cl]^+$; 384 (10%), $[Pd(L)]^{2+}$. Anal. Calc. for $C_{16}H_{11}N_3O_2PdCl_2$ (454.6 g mol^{-1}): C 42.27, H 2.44, N 9.24. Found: C 42.34, H 2.15, N 9.19.

Copper(II) complex (5). An ethyl acetate solution (10 mL) of $CuCl_2 \cdot 2H_2O$ (0.1 mmol, 17 mg) was added dropwise to a stirred ethyl acetate solution (10 mL) of ligand **1** (0.1 mmol, 28 mg) at room temperature. The reaction mixture was refluxed for 24 h. The solid product was precipitated as dark green crystals. The stable complex was filtered off, washed with ethyl acetate, diethyl ether, and dried; 22 mg yield (53%), mp 319.1–321.3 °C, IR spectrum in CsI, selected bands, cm^{-1} : 1749 (C=O), 1615 (C=N), 457 (Cu–N), 302 (Cu–Cl). Anal. Calc. for $C_{32}H_{22}N_6O_4Cu_2Cl_4$ (823.2 g mol^{-1}): C 46.68, H 2.69, N 10.21. Found C 46.31, H 2.24, N 10.26.

Computational details

All calculations were performed at the DFT level of theory as described earlier for palladium complexes.²¹ Gas phase geometry optimizations were performed with the Gaussian03 package³⁰ using the mPW1PW91 functional³¹ in ECP LanL2DZ basis set.³² Values of log P were obtained from the free Gibbs energies of structures optimized using CPCM continuum solvent models of water and 1-octanol using B3LYP functional and the same basis set. For 1-octanol the dielectric constant of 10.3 and the solvent radius (R_{solv}) of 0.2 were used. All calculations were carried out using default convergence criteria. Vibrational analysis was performed to confirm that all obtained structures correspond to stationary points.

X-Ray crystal structure determinations of 3 and 5

X-Ray crystal data were collected at 200 K with a Nonius KappaCCD diffractometer equipped with a rotating anode and graded multilayer X-ray optics to obtain monochromated Mo- $K\alpha$ radiation ($\lambda = 0.71073$ Å). The structures were solved with direct methods³³ and refined with SHELXL-97 by full-matrix least-squares on F^2 .³⁴ All non-hydrogen atoms were refined anisotropically, the hydrogen atoms were fixed in ideal geometry and allowed to ride on their parent atoms. The crystal data and X-ray details are given in Table 6.

Cell and cytotoxicity assay

Cell cultures. Human skin melanoma WM-115 cells as well as human leukemia promyelocytic HL-60 and lymphoblastic NALM-6 cell lines were used. Leukemia cells were cultured in

Table 6 Crystallographic data for **3** and **5**

	3	5
Net formula	$C_{16}H_{11}Cl_2N_3O_2Pd$	$C_{32}H_{22}Cl_4Cu_2N_6O_4$
$M_r/g\ mol^{-1}$	454.60	823.44
Crystal size/mm	$0.15 \times 0.09 \times 0.02$	$0.06 \times 0.04 \times 0.02$
T/K	200(2)	200(2)
Radiation	Mo- $K\alpha$	Mo- $K\alpha$
Diffractometer	KappaCCD	KappaCCD
Crystal system	Monoclinic	Triclinic
Space group	$P2_1/c$	$P\bar{1}$
$a/\text{\AA}$	9.5751(2)	8.4188(4)
$b/\text{\AA}$	24.2068(4)	9.2762(4)
$c/\text{\AA}$	7.00870(10)	10.6495(5)
$\alpha/^\circ$	90	83.019(2)
$\beta/^\circ$	105.1538(8)	87.266(2)
$\gamma/^\circ$	90	70.3459(16)
$V/\text{\AA}^3$	1568.01(5)	777.39(6)
Z	4	1
$D_c/g\ cm^{-3}$	1.92575(6)	1.75897(14)
μ/mm^{-1}	1.538	1.762
Refls. measured	6706	9991
R_{int}	0.0206	0.0846
Mean $\sigma(I)/I$	0.0389	0.0687
θ range/ $^\circ$	3.34–27.48	3.20–25.00
Observed refls.	2706	2156
x, y (weighting scheme)	0.0401, 0.0500	0.0400, 0.1154
Refls. in refinement	3560	2716
Parameters	218	218
$R(F_{obs})$	0.0295	0.0397
$R_w(F^2)$	0.0782	0.0956
S	1.064	1.051
Shift/error $_{max}$	0.001	0.001
Max. $\Delta\rho/e\ \text{\AA}^{-3}$	1.003	0.446
Min. $\Delta\rho/e\ \text{\AA}^{-3}$	–0.743	–0.504

RPMI 1640 (Invitrogen, Paisley, UK) medium supplemented with 10% fetal bovine serum and antibiotics (100 $\mu g\ ml^{-1}$ streptomycin and 100 U ml^{-1} penicillin). For melanoma WM-115 cells Dulbecco's minimal essential medium (DMEM) instead of RPMI 1640 was used. Normal cells, human umbilical vein endothelial cells (HUVECs) were grown in M 200 medium supplemented with 2% foetal bovine serum (FBS), epidermal growth factor (10 ng ml^{-1}) and antibiotics. HUVECs, M 200 medium and supplements were purchased from Cascade Biologics Inc, Mansfield, UK. Cells were grown in 37 °C in a humidified atmosphere of 5% CO_2 in air.

Cytotoxicity assay by MTT. Cytotoxicity of ligand **1**, its complexes **2–5** and cisplatin was determined by the MTT [3-(4,5-dimethylthiazol-2-yl)-2,5-diphenyltetrazolium bromide, Sigma, St. Louis, MO] assay as described in detail elsewhere.³⁵ Briefly, after 46 h of incubation with the drugs, the cells were treated with the MTT reagent and incubation was continued for 2 h. MTT-formazan crystals were dissolved in 20% SDS and 50% DMF at pH 4.7 and absorbance was measured at 562 and 630 nm on an ELISA-plate reader (ELX 800, Bio-Tek, USA). The values of IC_{50} (the concentration of test compound required to reduce the cells survival fraction to 50% of the control) were calculated from concentration–response curves and used as a measure of cellular sensitivity to a given treatment. Complexes and cisplatin were tested for their cytotoxicity in a final concentration 10^{-7} – 10^{-3} M. As a control, cultured cells were grown in the absence of drugs.

Data points represent means of at least 12 individual measurements \pm S.D.

Acknowledgements

Financial support from KBN (NN 405 428434 to E. B.) and the access to supercomputing facilities at Cyfronet, Cracow, ICM Warsaw and PCSS Poznan, Poland are gratefully acknowledged.

References

- 1 A. Daponte, P. A. Ascierto, A. Grabina, M. Melucci, S. Scala, A. Ottaiano, E. Simeone, G. Palmiers and G. Colella, *Anticancer Res.*, 2005, **25**, 1441–1447.
- 2 J. Gawlik, J. Zychowicz, A. Tudaj and H. Podbielska, *Terapia*, 2005, **163**, 49–51.
- 3 W. Kycler, P. Łaski, M. Porzegowski and M. Teresiak, *Współczesna Onkol.*, 2006, **10**, 175–178.
- 4 W. Ruka, Czerniak skóry, in *Onkologia Kliniczna*, ed. M. Krzakowski, Borgis Wydawnictwo Medyczne, Warszawa, 2001, vol. 1, 290.
- 5 M. Krzakowski, *Współczesna Onkol.*, 2003, **7**, 604–610.
- 6 E. Budzisz, *Wiad. Chem.*, 2007, **61**, 643–658.
- 7 B. Barszcz, *Coord. Chem. Rev.*, 2005, **249**, 2259–2276.
- 8 L. F. Szczepura, L. M. Witam and K. J. Takeuchi, *Coord. Chem. Rev.*, 1998, **174**, 5–32.
- 9 G. B. Onoa, V. Moreno, M. Font-Bardia, X. Solans, J. M. Perez and C. Alonso, *J. Inorg. Biochem.*, 1999, **75**, 205–212.
- 10 M. S. Chande, N. V. Thakkar and D. V. Patil, *Drug Res.*, 1999, **56**, 207–210.
- 11 D. C. G. A. Pinto, A. M. S. Silva, J. A. S. Cavaleiro, C. Foces-Foces, A. L. Llamas-Saiz, N. Jagerovic and J. Elguero, *Tetrahedron*, 1999, **55**, 10187–10200.
- 12 A. Cameron Church, M. U. Koller, S. A. O'Grady and C. F. Beam, *Synth. Commun.*, 1996, **26**, 2603–2611.
- 13 G. Pallazino, L. Cecchi, F. Melani, V. Colotta, G. Filacchioni, C. Martini and A. Lucachini, *J. Med. Chem.*, 1987, **30**, 1737–1742.
- 14 K. Wang, J. Lu and R. Li, *Coord. Chem. Rev.*, 1996, **151**, 53–88.
- 15 S. Mylonas, A. Valavanidis, K. Dimitropoulos, M. Polissiou, A. S. Tsietsoglou and I. S. Vizirianakis, *J. Inorg. Biochem.*, 1988, **34**, 265–275.
- 16 E. Budzisz, B. K. Keppler, G. Giester, M. Woźniczka, A. Kufelnicki and B. Nawrot, *Eur. J. Inorg. Chem.*, 2004, **22**, 4412–4419.
- 17 M. D. Hall and T. W. Hambley, *Coord. Chem. Rev.*, 2002, **232**, 49–67.
- 18 S. M. Kupchan, M. A. Eakin and A. M. Thomas, *J. Med. Chem.*, 1971, **14**, 1147–1152.
- 19 A. Kufelnicki, M. Woźniczka, L. Checinska, M. Miernicka and E. Budzisz, *Polyhedron*, 2007, **26**, 2589–2596.
- 20 M. Miernicka, A. Szulawska, M. Czyz, I.-P. Lorenz, P. Mayer, B. Karwowski and E. Budzisz, *J. Inorg. Biochem.*, 2008, **102**, 157–165.
- 21 E. Budzisz, M. Malecka, I.-P. Lorenz, P. Mayer, P. Paneth, R. Kwiecien, U. Krajewska and M. Rozalski, *Inorg. Chem.*, 2006, **45**, 9688–9695.
- 22 R. Wysokiński and D. Michalska, *J. Comput. Chem.*, 2001, **22**, 901–912.
- 23 J. A. Platts, S. P. Oldfield, M. M. Reif, A. Palmucci, D. Gabano and E. Osella, *J. Inorg. Biochem.*, 2006, **100**, 1199–1207.
- 24 R. S. Mülliken, *J. Chem. Phys.*, 1955, **23**, 1833–1840.
- 25 A. E. Reed, R. B. Weinstock and F. Weinhold, *J. Chem. Phys.*, 1985, **83**, 735–746.
- 26 B. H. Besler, M. Kenneth, Jr and P. A. Kollman, *J. Comput. Chem.*, 1990, **11**, 431–439.
- 27 B. Szewczyk, W. A. Sokalski and J. Leszczyński, *J. Chem. Phys.*, 2002, **117**, 6952–6958.
- 28 K. Jozwiak, H. Szumilo and E. Soczewinska, *Wiad. Chem.*, 2001, **55**, 1047.
- 29 B. T. Khan, J. Bhatt, K. Najmuddin, S. Shamsuddin and K. Annapoorna, *J. Inorg. Biochem.*, 1991, **44**, 55.
- 30 M. J. Frisch, G. W. Trucks, H. B. Schlegel, G. E. Scuseria, M. A. Robb, J. R. Cheeseman, J. A. Montgomery, Jr., T. Vreven, K. N. Kudin, J. C. Burant, J. M. Millam, S. S. Iyengar, J. Tomasi, V. Barone, B. Mennucci, M. Cossi, G. Scalmani, N. Rega, G. A. Petersson, H. Nakatsuji, M. Hada, M. Ehara, K. Toyota, R. Fukuda, J. Hasegawa, M. Ishida, T. Nakajima, Y. Honda, O. Kitao, H. Nakai, M. Klene, X. Li, J. E. Knox, H. P. Hratchian, J. B. Cross, V. Bakken, C. Adamo, J. Jaramillo, R. Gomperts, R. E. Stratmann, O. Yazyev, A. J. Austin, R. Cammi, C. Pomelli, J. Ochterski, P. Y. Ayala, K. Morokuma, G. A. Voth, P. Salvador, J. J. Dannenberg, V. G. Zakrzewski, S. Dapprich, A. D. Daniels, M. C. Strain, O. Farkas, D. K. Malick, A. D. Rabuck, K. Raghavachari, J. B. Foresman, J. V. Ortiz, Q. Cui, A. G. Baboul, S. Clifford, J. Cioslowski, B. B. Stefanov, G. Liu, A. Liashenko, P. Piskorz, I. Komaromi, R. L. Martin, D. J. Fox, T. Keith, M. A. Al-Laham, C. Y. Peng, A. Nanayakkara, M. Challacombe, P. M. W. Gill, B. G. Johnson, W. Chen, M. W. Wong, C. Gonzalez and J. A. Pople, *GAUSSIAN 03 (Revision D.01)*, Gaussian, Inc., Wallingford, CT, 2004.
- 31 C. Adamo and V. Barone, *J. Chem. Phys.*, 1998, **108**, 664–675.
- 32 P. J. Hay and W. R. Wadt, *J. Chem. Phys.*, 1985, **82**, 270–298.
- 33 A. Altomare, M. C. Burla, M. Camalli, G. L. Cascarano, C. Giacovazzo, A. Guagliardi, A. G. G. Moliterni, G. Polidori and R. Spagna, *J. Appl. Crystallogr.*, 1999, **32**, 115–119.
- 34 SHELXL-97 (G. M. Sheldrick. University of Göttingen, 97-2 version), 1997.
- 35 E. Budzisz, U. Krajewska, M. Rozalski, A. Szulawska, M. Czyz and B. Nawrot, *Eur. J. Pharmacol.*, 2004, **502**, 59–65.